Tissue Engineering

Tissue Engineering Manuscript Central: http://mc.manuscriptcentral.com/ten

Comparative study of immunodeficient rat strains in engraftment of hiPSC-derived airway epithelia

Journal:	*Tissue Engineering*
Manuscript ID	TEA-2023-0214.R1
Manuscript Type:	Original Article - Part A
Date Submitted by the Author:	n/a
Complete List of Authors:	Hayashi, Yasuyuki; Kyoto University Graduate School of Medicine Faculty of Medicine, Otolaryngology, Head and Neck Surgery Ohnishi, Hiroe; Kyoto University Graduate School of Medicine Faculty of Medicine, Otolaryngology, Head and Neck Surgery Kitano, Masayuki; Kyoto University Graduate School of Medicine Faculty of Medicine, Otolaryngology, Head and Neck Surgery Kishimoto, Yo; Kyoto University Graduate School of Medicine Faculty of Medicine, Otolaryngology, Head and Neck Surgery Takezawa, Toshiaki; Chiba Institute of Science, Faculty of Pharmacy Okuyama, Hideaki; McGill University Faculty of Medicine and Health Sciences, School of Communication Sciences and Disorders Yoshimatsu, Masayoshi; Kagoshima University Graduate School of Medicine and Dental Sciences, Otolaryngology, Head and Neck Surgery Kuwata, Fumihiko; Kyoto University, Department of Otolaryngology-Head and Neck Surgery Tada, Takeshi; Georgia State University Institute for Biomedical Sciences Mizuno, Keisuke; Kyoto University Graduate School of Medicine Faculty of Medicine, Otolaryngology, Head and Neck Surgery Omori, Koichi; Kyoto University Graduate School of Medicine Faculty of Medicine, Otolaryngology, Head and Neck Surgery
Keyword:	IPS Cells < Fundamentals of Tissue Engineering (DO NOT select this phrase; it is a header ONLY), Trachea < Applications in Tissue Engineering (DO NOT select this phrase; it is a header ONLY), Cell Differentiation < Fundamentals of Tissue Engineering (DO NOT select this phrase; it is a header ONLY)
Manuscript Keywords (Search Terms):	hiPSC, airway epithelial cell, transplantation, Trachea regeneration, immunodeficient rat
Abstract:	The airway epithelia (AE) play a role in the clearance of foreign substances through ciliary motility and mucus secreted. We developed an artificial trachea that is made of collagen sponges and polypropylene mesh for the regeneration of the tracheal defect, and it was used for a clinical study. Then, a model in which the luminal surface of an artificial trachea covered with a human-induced pluripotent stem cell-derived AE (hiPSC-AE) was transplanted into the tracheal defect of nude rats to promote epithelialization. In the future, this model was expected to be applied to research on infectious diseases and drug discovery as a trachea-humanized rat model. However, at present, sufficient engraftment has not been achieved to evaluate functional recovery in

transplanted cells. Therefore, this study focused on immunosuppression in recipient rats. Nude rats lack T-cell function and are widely used for transplantation experiments; however, more severe immunosuppressed recipients are preferred for xenotransplantation. Several strains of immunodeficient rats were created as rats that exhibit more severe immunodeficiency until now. In this study, to establish a trachea-humanized rat model in which human AE function can be analyzed to improve engraftment efficiency, engraftment efficiency in nude rats and X-linked severe combined immunodeficiency (X-SCID) rats following hiPSC-AE transplantation was compared. In the analysis of the proportion of engrafted cells in total cells at the graft site, the engraftment efficiency of epithelial cells tended to be high in X-SCID rats, although no statistical difference was found between the two groups, whereas the engraftment efficiency of mesenchymal cells was higher in X-SCID rats. Furthermore, the number of immune cells that accumulated in the grafts showed that a pan T-cell marker, i.e., CD3-positive cells, did not differ between the two strains; however, CD45-positive cells and major histocompatibility complex (MHC) class II-positive cells significantly decreased in X-SCID rats. These results indicate that X-SCID rats are more useful for the transplantation of hiPSC-AE into the tracheae to generate trachea-humanized rat models.

Comparative study of immunodeficient rat strains in engraftment of hiPSC-derived airway epithelia

Running title: Comparison of rat strains in hiPSC-AE engraftment

Yasuyuki Hayashi, MD[1], Hiroe Ohnishi, PhD[1], Masayuki Kitano, MD[1], Yo Kishimoto, MD, PhD[1*], Toshiaki Takezawa, PhD[2,6], Hideaki Okuyama, MD, PhD[3], Masayoshi Yoshimatsu, MD, PhD[1,4], Fumihiko Kuwata, MD, PhD[1], Takeshi Tada, MD, PhD[5], Keisuke Mizuno, MD[1], Koichi Omori, MD, PhD[1]

*Corresponding Author: Yo Kishimoto
Department of Otolaryngology–Head and Neck Surgery
Graduate School of Medicine, Kyoto University
54 Shogoin Kawahara-cho, Sakyo-ku, Kyoto City
Kyoto 606-8507, Japan.
Telephone: +81-75-751-3346
Fax: +81-75-751-7225
E-mail: y_kishimoto@ent.kuhp.kyoto-u.ac.jp

[1] Department of Otolaryngology–Head and Neck Surgery, Graduate School of medicine, Kyoto University, 54 Kawahara-cho, Shogoin, Sakyo-ku, Kyoto City, Kyoto, 606-8507, Japan

[2] Faculty of Pharmacy, Chiba Institute of Science, 15-8 Shiomi-cho, Choshi City, Chiba, 288-0025, Japan

[3] School of Communication Sciences and Disorders, Faculty of Medicine and Health Sciences, McGill University, Montreal, Canada

[4] Department of Otolaryngology, Head and Neck Surgery, Graduate School of Medical and Dental Sciences, Kagoshima University, 35-1 Sakuragaoka 8 chome, Kagoshima 890-8544, Japan

[5] Center for Inflammation, Immunity & Infection Institute for Biomedical Sciences Georgia State University, Atlanta, GA 30303-5035, USA

[6] Institute of Agrobiological Sciences, National Agriculture and Food Research Organization, 1-2 Owashi, Tsukuba City, Ibaraki 305-8634, Japan

Yasuyuki Hayashi (Tel: +81-75-751-3346, Mail: yasuyuki_hayashi@ent.kuhp.kyoto-u.ac.jp)

Hiroe Ohnishi (Tel: +81-75-751-3346, Mail: h_oonishi@ent.kuhp.kyoto-u.ac.jp)

Masayuki Kitano (Tel: +81-75-751-3346, Mail: kitano_masayuki@ent.kuhp.kyoto-u.ac.jp)

Yo Kishimoto (Tel: +81-75-751-3346, Mail: y_kishimoto@ent.kuhp.kyoto-u.ac.jp)

Toshiaki Takezawa (Tel: +81-479-30-4619, Mail: ttakezawa@cis.ac.jp)

Hideaki Okuyama (Tel: +1-514-398-5933, Mail: h_okuyama@ent.kuhp.kyoto-u.ac.jp)

Masayoshi Yoshimatsu (Tel: +81-99-275-5410, Mail: m_yoshimatsu@ent.kuhp.kyoto-u.ac.jp)

Fumihiko Kuwata (Tel: +81-75-751-3346, Mail: f_kuwata@ent.kuhp.kyoto-u.ac.jp)

Takeshi Tada (Tel: +1-404-413-3581, Mail: ttada@gsu.edu)

Keisuke Mizuno (Tel: +81-75-751-3346, Mail: k_mizuno@ent.kuhp.kyoto-u.ac.jp)

Koichi Omori (Tel: +81-75-751-3343, Mail: omori@ent.kuhp.kyoto-u.ac.jp)

Keywords: hiPSC, airway epithelial cell, transplantation, Trachea regeneration, immunodeficient rat

Abstract

The airway epithelia (AE) play a role in the clearance of foreign substances through ciliary motility and mucus secreted. We developed an artificial trachea that is made of collagen sponges and polypropylene mesh for the regeneration of the tracheal defect, and it was used for a clinical study. Then, a model in which the luminal surface of an artificial trachea covered with a human-induced pluripotent stem cell-derived AE (hiPSC-AE) was transplanted into the tracheal defect of nude rats to promote epithelialization. In the future, this model was expected to be applied to research on infectious diseases and drug discovery as a trachea-humanized rat model. However, at present, sufficient engraftment has not been achieved to evaluate functional recovery in transplanted cells. Therefore, this study focused on immunosuppression in recipient rats. Nude rats lack T-cell function and are widely used for transplantation experiments; however, more severe immunosuppressed recipients are preferred for xenotransplantation. Several strains of immunodeficient rats were created as rats that exhibit more severe immunodeficiency until now. In this study, to establish a trachea-humanized rat model in which human AE function can be analyzed to improve engraftment efficiency, engraftment efficiency in nude rats and X-linked severe combined immunodeficiency (X-SCID) rats following hiPSC-AE transplantation was compared. In the analysis of the proportion of engrafted cells in total cells at the graft site, the engraftment efficiency of epithelial cells tended to be high in X-SCID rats, although no statistical difference was found between the two groups, whereas the engraftment efficiency of mesenchymal cells was higher in X-SCID rats. Furthermore, the number of immune cells that accumulated in the grafts showed that a pan T-cell marker, i.e., CD3-positive cells, did not differ between the two strains; however, CD45-positive cells and major histocompatibility complex (MHC) class II-positive cells significantly decreased in X-SCID rats. These results indicate that X-SCID rats are more useful for the transplantation of hiPSC-AE into the tracheae to generate trachea-humanized rat models.

Impact statement

The models to investigate the pathological mechanism and effect of medicines are important. In the tracheae, since cells are constantly exposed to the airflow in respiration, replicating in vivo conditions with cultured cells in vitro is difficult. Therefore, to establish a trachea-humanized rat, a model in which hiPSC-AE were transplanted into the tracheal defect of nude rats was generated. To use this model as a trachea-humanized model, higher engraftment efficiency is required. This study indicated that X-linked severe combined immunodeficiency rats are superior to nude rats as recipients. These results will contribute to the establishment of trachea-humanized rats.

Introduction

Since the first establishment in 2007,[1] various regenerative strategies using human-induced pluripotent stem cells (hiPSCs) have been developed, and it has allowed the generation of cells that constitute various tissues and organs from all cells in the human body. Several cell types such as retinal pigment epithelial cells, dopaminergic progenitor cells, platelets, and cardiomyocytes have been generated from hiPSCs and used in clinical research.[2–5] Other cell types generated from hiPSCs were transplanted into mice, rats, monkeys, and other animals in preclinical studies or basic research.

Regarding airway epithelia (AE), several induction methods from hiPSCs have been established by some groups, and hiPSC-derived AE (hiPSC-AE) induced by these methods exhibit similar morphology and function to biological AE.[6,7] By using one of these induction protocols,[7] we performed a transplantation study using an artificial trachea covered with a hiPSC-AE sheet into the tracheal defects of nude rats and monitored hiPSC-AE on the luminal surface of the trachea for up to 2 weeks after the transplantation.[8] However, the proportion of surviving epithelia~~l cells~~ in all epithelia~~l cells~~ in the transplanted area at 1 and 2 weeks after the transplantation were 8.5% and 14.3%, respectively.[8] In basic studies for cell transplantation treatment or in generating trachea-humanized rats for the research of tracheal diseases, a high survival rate is necessary.

In xenotransplantation, one of the factors critical for the achievement of a high survival rate is the regulation of immune response in recipient animals. Immunosuppressive agents or immunodeficient animals are widely used to increase the survival rate of transplanted cells. In a previous study, nude

rats, which exhibit deficient T-cell function caused by the lack of normal thymuses due to the mutation in the *Foxn1* gene,[9] have been used as immunodeficient recipient animals.[8] Recently, severe combined immunodeficiency (SCID) rats were generated using CRISPR/Cas9 genome editing by causing in the mutation of the *interleukin-2 receptor gamma chain* gene (*Il2rg*) in F344/Jcl rats. These rats had severe thymic hypoplasia and a significantly lower white blood cell count due to a decrease in lymphocytes, but red blood cells in peripheral blood were unaffected. In addition, flow cytometry analysis revealed a markedly reduced number of T, B, and natural killer cells.~~Recently, rats with X-linked severe combined immunodeficiency (X-SCID) were reported using the CRISPR/Cas9 genome-editing system.[10] These rats have a mutation in the gene encoding the interleukin 2 receptor gamma (Il2rg), which results in loss of function.[10] *Il2rg* is a gene coding an essential component of the IL2 receptor and was identified as the responsible gene for X-SCID.[11] X-SCID rats show immunodeficient phenotypes characterized as a nearly complete lack of T, B, and natural killer (NK) cells.~~[10] Therefore, this X-SCID rat~~s~~ strain is~~are~~ preferred for xenotransplantation.

In this study, we compared the efficiency of the engraftment in nude and X-SCID rats following transplantation of hiPSC-AE to achieve a high survival rate with aims of establishing methods of cell transplantation treatment and generating humanized rats for the research of tracheal diseases.

Materials and methods

hiPSC culture and AE induction

The hiPSC line 253G1,[12] obtained from RIKEN BioResource Research Center, was used for AE induction as previously described.[7,13] The cells were maintained on dishes coated with Geltrex (Thermo Fisher Scientific, Waltham, MA, USA) in Essential 8 medium (Thermo Fisher Scientific).

The induction of AE from hiPSCs comprised six steps. In step 1, undifferentiated hiPSCs were seeded on Geltrex-coated plates containing the RPMI1640 medium (Nacalai Tesque, Kyoto, Japan), 1 × B27 supplement (Thermo Fisher, Kanagawa, Japan), 50 U/mL of penicillin/streptomycin (Thermo Fisher Scientific), 100 ng/mL of human activin A (R&D System, Minneapolis, MN, USA), 1 μM of CHIR99021 (Axon Medchem, Groningen, Netherlands), 10 μM of Y27632 (FUJIFILM Wako Pure

Chemical Corporation, Osaka, Japan) (days 0–1), and 0.25 mM (day 1) or 0.125 mM (days 2–4) of sodium butyrate (FUJIFILM Wako) were used to induce the endoderm cells. From days 6–28 (steps 2–4), the basal medium was composed of DMEM/F-12 with GlutaMAX (Thermo Fisher Scientific), 1 × B27 supplement, 50 U/mL of penicillin/streptomycin, 0.05 mg/mL of L-ascorbic acid (FUJIFILM Wako), and 0.4 mM of monothioglycerol (FUJIFILM Wako Pure Chemical Corporation). In step 2, endoderm cells were differentiated into anterior foregut endoderm cells by culture in the basal medium supplemented with 100 ng/mL of human recombinant noggin (Human Zyme, Chicago, IL, USA) and 10 μM of SB431542 (Selleck Chemicals, Houston, TX, USA) for 4 days (from days 6 to 9). In step 3 (from days 10 to 13), the cells were cultured in the basal medium supplemented with 20 ng/mL of human recombinant BMP4 (Human Zyme), 2.5 μM of CHIR99021, and 0.1 μM of all-trans retinoic acid (Sigma-Aldrich, St. Louis, MO, USA) to induce ventralized anterior foregut endoderm cells (VAFECs) from anterior foregut endoderm cells. On day 14, VAFECs were purified by magnetic-activated cell sorting using mouse anti-human CPM antibodies (FUJIFILM Wako Chemical Corporation), which labels NKX2-1+ cells. CPM+ cells were embedded in the step 4 medium (basal medium, 3.0 μM of CHIR99021, 100 ng/mL of FGF10 [FUJIFILM Wako Chemical Corporation], and 10 μM of Y27632) and growth factor-reduced Matrigel (Corning, Corning, NY, USA) at a ratio of 1:1 and maintained on a 12-well cell culture insert with PET membrane (Corning, #353292) for 14 days (days 14 to 27). To generate proximal AE progenitor cell spheroids, on day 28, cells were cultured in the step 5 medium consisting of PneumaCult-ALI Maintenance medium (STEMCELL Technologies, Vancouver, Canada), 10 μM of Y27632, 4 μg/mL of heparin (Nacalai Tesque), 1 μM of hydrocortisone (Sigma-Aldrich), and 10 μM of DAPT (FUJIFILM Wako Chemical Corporation). On day 42, single-cell suspension was obtained from the spheroids by enzymic treatment and seeded on a cell culture insert. In step 6, cells were seeded on culture inserts with collagen vitrigel membrane (ad-MED vitrigel; Kanto Chemical, Tokyo, Japan) or atelocollagen vitrigel membrane and cultured in the ALI condition for 14 days to lead AE differentiation in the form of a monolayer cell sheet. For transplantation experiments, these hiPSC-AEs on vitrigel membranes were used as hiPSC-AE sheets.

Preparation of the artificial trachea

The collagen (Nippon Meat Packers, Inc., Osaka, Japan) was dissolved in pure water (6 mg/mL), adjusted to pH 7, and centrifuged to obtain the pellet. Then, the collagen pellet was frozen at −80°C and lyophilized for 10 days. The dried collagen was then cut into small pieces, dissolved in ultrapure water (106.4 mg/mL) while HCl was added, and adjusted to pH 3. The collagen solution was poured into a mold, a polypropylene mesh coated with the collagen solution was put on, an equal volume of the collagen solution was poured, and then it was frozen at −80°C overnight. After lyophilization for 1 week, collagen including polypropylene mesh was crosslinked by heating, sterilized by EOC gas, and stored in a desiccator.

Electron microscopy

Cells were fixed with a phosphate-buffered solution (PBS) with 4% paraformaldehyde (PFA) and 2% glutaraldehyde overnight at 4°C, incubated in 1% osmium tetroxide for 2 h, and dehydrated by ascending concentrations of ethanol. For scanning electron microscopy (SEM), dehydrated cells were dried using the critical point drying method and coated with a thin layer of platinum palladium. For transmission electron microscopy (TEM), dehydrated cells were embedded in epoxy resin and DMP-30. Thin sections were stained with uranyl acetate and lead citrate. The specimens were observed using the scanning electron microscope S-4700 (Hitachi C., Tokyo, Japan) or the transmission electron microscope H7650 (Hitachi).

Rats

Wild-type rats (F344, CLEA Japan, Osaka, Japan), nude rats (F344/NJcl.Cg-*Foxn1*^{rnu}, CLEA Japan, Osaka, Japan), and X-linked immunodeficient (X-SCID) rats (F344-*Il2rge*^{m1lexas}, NBRP No. 0883) provided by the National BioResource Project Rats were used for the transplantation experiments. Wild-type rats were 12–14 weeks old and weighed 200–305 g, nude rats were 8–11 weeks old and weighed 180–240 g, and X-SCID rats were at 8–12 weeks old and weighed 180–240 g. All rats used in this study were male. The animal experimental protocol was approved by the Animal Research

Committee of the Graduate School of Medicine, Kyoto University (Med Kyo 23113).

Transplantation

Transplantation study was performed using 6 wild-type rats (for positive control for immune cell immunostaining), 18 nude rats (8 rats for comparison of engraftment efficiency and 10 for vitrigel membrane examination), and 8 X-SCID rats. The transplantation experiments were performed under anesthesia with intraperitoneal injection of a mixture of midazolam (2 mg/kg), butorphanol (2.5 mg/kg), and medetomidine (0.15 mg/kg). The trachea was exposed through a midline neck skin incision and separation of the bilateral sternohyoid and sternothyroid muscles. A square tracheal defect was created in each rat by incision with a scalpel. The defect size was approximately 2.5 mm (two tracheal rings) in length and 2 mm in width. The grafts that contained the artificial trachea and were covered in the luminal side with hiPSC-AE sheet were placed over the tracheal defects. Then, the sternohyoid and sternothyroid muscles and incised skin were sutured. All rats were euthanized with carbon dioxide 2 weeks after transplantation, and the tracheae were collected and used for subsequent histological examinations.

Immunofluorescent staining

Induced cells were fixed with 4% PFA for 15 min at room temperature (RT). After washing with PBS, cells were permeabilized with 0.2% Triton for 5 min at RT and were incubated with 1% bovine serum albumin (BSA) in PBS for 10 min at RT. Then, cells were incubated with primary antibodies (Table 1) overnight at 4°C, washed with PBS, and incubated with Alexa Fluor-conjugated secondary antibodies for 1 h at RT. Nuclei were labeled with 4',6-diamidino-pa2-phenylindole (DAPI; Thermo Fisher Scientific). The tracheae transplanted with hiPSC-AE including the sternohyoid and sternothyroid muscles, and section of cell sheet were immersed in 4% PFA for 1 day. Subsequently, they were immersed in 10%, 20%, and 30% sucrose for 8 h each and embedded in an optimal cutting temperature compound (Sakura Finetek Japan, Tokyo, Japan). The embedded tissues were sliced into 10 µm-thick sections. From each rat, 10-20 sections at 100-µm intervals were used for staining. After

drying, the sections were incubated with PBS for 5 min at RT and were permeabilized with 0.2% Triton for 5 min at RT. After blocking with 1% BSA in PBS, the sections were incubated with primary antibodies (Table 1), washed with PBS, incubated with Alexa Fluor-conjugated secondary antibodies, Alexa Fluor-conjugated phalloidin (sc-363797, Santa Cruz, Dallas, TX, USA), and DAPI for 1 h at RT, washed with PBS, and mounted using Fluoromount-G® Anti-Fade (Southern Biotechnology Associates Inc., Birmingham, AL, USA). Specimens were observed, and images were obtained using a BIOREVO BZ-9000 fluorescence microscope (KEYENCE, Osaka, Japan). For the analyses of mesenchymal cells, binary images were generated from immunofluorescent images of Human Nuclear Antigen (HNA)-positive areas and grafted areas~~.~~

Statistical analysis

The survival rate of hiPSC-derived epithelia, area of hiPSC-derived mesenchymal cells, and number of each immune cell in the graft were compared between the two groups of X-SCID and nude rats using the Mann–Whitney U test. Data are expressed as median (range, minimum–maximum value), and p-values of <0.05 were considered statistically significant.

Results

Preparation of grafts using artificial tracheae and hiPSC-AE sheets

After hiPSC-AE induction from 253G1 line iPSCs on collagen vitrigel membrane, ~~ciliated cell marker~~ acetylated-alpha-tubulin (AcTub)-~~expressing~~ positive ciliated cells were observed in ~~an epithelial marker, i.e.,~~ the E-cadherin-~~expressing~~ positive epithelia (Fig. 1A). In the vertical sections of cell sheets, cytokeratin5 (KRT5)-positive basal cells and Mucin5AC (MUC5AC)-positive goblet cells were also observed (Fig. 1B, C) Cilia-like structures were also observed by ~~SEM~~ TEM (Fig. 1D~~B~~) and ~~transmission electron microscopy~~SEM (Fig. ~~1C~~1E). In TEM images, which are composed of nine doublet microtubules arranged in a circle around two central singlet microtubules with dynein arms known as a specific motif in motile cilia (Fig. ~~1C~~1~~E~~D, inset). These observations revealed that hiPSC-AE were induced from the 253G1 cell line, as reported previously. A cross-sectional SEM

image of the artificial trachea showed that a polypropylene mesh was embedded in the middle of the collagen sponge (Fig. ~~1D~~1F). These results suggest that the hiPSC-AE sheets and artificial trachea were prepared as in previous studies.

Transplantation of hiPSC-AE into immunodeficient rats

A schema of the transplantation is shown in Fig. 2A. An artificial trachea covered with an hiPSC-AE sheet was transplanted into the tracheal defect. Cell survival rates were calculated using cross-sections of tracheae including the transplanted areas 2 weeks after transplantation (Fig. 2B). The proportion of the hiPSC-derived epithelia in total epithelia at the transplanted area was calculated from two epithelial areas with a width of 350 μm at the center and one side of the tracheal defect area (Fig. 2B, two yellow squares). The proportion of hiPSC-derived mesenchymal cells was calculated from the HNA-positive and grafted areas (Fig. 2B, area surrounded by the yellow dotted line).

Comparison of cell survival rates in nude and X-SCID rats

HNA-positive hiPSC-derived epithelial cells were confirmed in five out of eight animals 2 weeks after transplantation in both nude and X-SCID rats (Fig. 3A). Some HNA-positive cells also expressed AcTub (Fig. 3Ac, f). The proportions of HNA-positive epithelia (Fig. 3Ab, e) in DAPI-positive epithelia (Fig. 3Ac, f) were examined to identify the engraftment efficiency in the epithelia. The median rates of the HNA-positive epithelia in the DAPI-positive epithelia in the grafted area were 1.6% (0.38%–4.38%) in nude rats (n = 5) and 2.27% (1.36%–9.04%) in X-SCID rats (n = 5), respectively (Fig. 3B). As a result, the engraftment efficiency of the epithelia tended to be high in X-SCID rats, although no statistical difference was found between the two groups (p = 0.35). On the contrary, HNA-positive hiPSC-derived mesenchymal cells were confirmed in all transplanted animals 2 weeks after transplantation in both nude and X-SCID rats (Fig. 4~~Ae, f~~A). The proportions of HNA-positive areas (Fig. 4~~A~~Ba, c, d, f) in DAPI-positive areas (Fig. 4~~A~~Bb, c, e, f) in the grafted area were examined to identify the engraftment efficiency in mesenchymal cells. The median rates of HNA-positive areas in the grafted areas were 0.63% (0.11%–3.32%) in nude (n = 8) and 3.6% (0.77%–

11.12%) in X-SCID (n = 8) rats. The engraftment efficiency of mesenchymal cells was statistically significantly higher in X-SCID rats (p = 0.02) (Fig. 4~~B~~C).

Immune responses in nude and X-SCID rats after transplantation

Furthermore, the immune cell accumulation in the transplanted areas was also compared. Wild-type rats transplanted artificial tracheae covered with collagen vitrigel sheets without hiPSC-AE were used as positive controls for immunostaining. The number of three types of immune cells, CD3-positive cells, CD45-positive cells, and MHC class II-positive cells, was examined (Fig. 5A). The number of each marker-positive cell in grafted areas was counted. The median counts of pan T-cell marker CD3-positive cells in nude and X-SCID rats were 3.33 (0.14–13.67) and 4.12 (0.7–13.63), respectively (nude rats, n = 8, X-SCID rats, n = 8) and did not differ between the two groups (p = 0.674) (Fig. 5B). In CD45-positive cells and MHC class II-positive cells including leukocytes other than T cells, the median counts of CD45-positive cells in nude and X-SCID rats were 73.26 (40.56–116.67) and 33.13 (15.45–76.75), respectively (nude rats, n = 8, X-SCID rats, n = 8), and the median counts of MHC class II-positive cells in nude and X-SCID rats were 64.75 (44.55–90.28) and 37.93 (22.6–73), respectively (nude rats, n = 8, X-SCID rats, n = 8) and significantly decreased in X-SCID rats (p = 0.005, CD45-positive cells; p = 0.009, MHC class II-positive cells) (Fig. 5B).

Discussion

The regeneration of AE in otorhinolaryngological tissues by hiPSC-AE transplantation has been studied; however, no studies have compared recipient rat strains in hiPSC-AE transplantation. Therefore, in this study, we compared engraftment efficiency and examined immune responses between nude and X-SCID rats to improve epithelialization by hiPSC-AE transplantation.

Xenotransplantation using immunodeficient animals is essential for the analysis of pathogenetic mechanisms and the development of cell transplantation therapies using human iPS cell-derived cells. As recipient animals for transplantation studies, NSG mouse (NOD.Cg-*Prkdc*^{scid} *Il2rg*^{tm1Wjl}) and NOG mouse (NOD.Cg-*Prkdc*^{scid} *Il2rg*^{tm1Sug}), which are deficient in T, B, and NK cells, innate immune

response, and others were established.[21]. As in this study, for studies requiring animals than larger mice, immunodeficient rats such as SCID,[22] X-SCID,[10,23] and FSG rats,[22] were also established. Furthermore, immunodeficient rabbits,[24] immunodeficient pigs,[25] and immunodeficient marmosets[26] were also reported as larger immunodeficient animals and are useful for preclinical studies.

Innate immune responses by NK cells, macrophages, and neutrophils are involved in graft rejection. These cells intricately interact with each other. By binding the immunocomplex of porcine cells and natural antibodies of human or non-human primates, NK cells and macrophages were activated, and antibody-dependent cellular cytotoxicity was induced against porcine cells. In addition, macrophages and NK cells were activated by the incompatibility between the SLA1 and NK receptors. The binding of damage-associated pattern molecules from dead cells to toll-like receptors, receptors for advanced glycation end-products, and macrophage-inducible C-type lectins activates macrophages, resulting in the induction of activation signals and release of various pro-inflammatory cytokines from macrophages. Then, released cytokines activate neutrophils and promote cell death. Furthermore, macrophages are activated by neutrophil extracellular traps from neutrophils. NK cells were activated by macrophages, and macrophages and neutrophils were activated by interferon-γ from NK cells.[18] Compared with nude rats lacking only T cells, X-SCID rats lacking T, B, and NK cells indicated that immune rejection in xenografts by these cells is suppressed in X-SCID rats, resulting in more efficient engraftment. In the NOG mouse mentioned above, a decrease in complement activity and macrophage dysfunction caused by a partial loss of innate immune function derived from the NOD lineage is confirmed, and they widely are used in xenotransplantation studies.[20] If a strain with such characteristics could be produced in rats, it would be useful for xenotransplantation.

Nude rats that arose spontaneously have been the most commonly used immunodeficient rats. The nude rats have a nonsense mutation (1429C > T) in the *Foxn1* gene[27] and exhibit an abnormal thymus rudiment. As a result, nude rats had depleted thymus-dependent areas in the spleen, mesentery, and popliteal lymph nodes and are characterized primarily by thymus-dependent immunodeficiency (T-cell dysfunction).[28] T cells are nearly depleted, whereas B and NK cells are normal in nude rats. For xenotransplantation, extremely immunodeficient rats were required. The development of genome-

editing techniques made it possible to generate mutant rats easily, and several immunodeficient rats were generated. In 2010, X-SCID rats were generated by the *Il2rg* locus, which is the gene responsible for X-SCID in humans and mice.[23] The mutation of genes that encode IL2RG, which plays an important role as a common gamma chain in signaling by interleukins (ILs) such as IL-2, IL-4, IL-7, IL-9, IL-15, and IL-21, leads to the lack of mature lymphocytes.[29] These rats showed abnormal lymphoid development, and T, B, and NK cells were markedly diminished, although some cells were present.[23] Moreover, rats that lack either the *Prkdc* gene (SCID) or the *Prkdc* and *Il2rg* (FSG) genes were generated using zinc-finger nucleases,[22] and rats were knocked out the *Il2rg* gene (X-SCID) alone or together with the recombination activating gene 2 (*Rag2*) (*Il2rg* and *Rag2* dKO) using the CRISPR/Cas9 genome-editing system.[10] T cells were absent from SCID rats, and B cells were absent from SCID and FSG rats. NK cells were present in the SCID but were mostly diminished in FSG rats.[22] In *Il2rg*-single knockout (sKO) and *Il2rg*/*Rag2*-double knockout (dKO) rats, the B and NK cell counts were markedly reduced in both knockout rats. By contrast, T-cell counts were markedly reduced, although some cells were present in only sKO rats.[10] In addition, Il2rg- sKO and *Il2rg*/*Rag2*-dKO rats do not exhibit growth retardation or gametogenesis defects, unlike SCID or FSG rats. Therefore, in this study, X-SCID (*Il2rg*-sKO) rats were donated from the National BioResource Project-Rat at Tokyo University (https://www.ims.u-tokyo.ac.jp/animal-genetics/scid/).

In some tissues, the effectiveness of the transplantation of human pluripotent stem cell (hPSC)-derived cells between nude and X-SCID rats was compared. In the transplantation of hPSC-derived dopaminergic (DA) neurons, no statistical differences were noted in MHC class II expression, B-cell and T-cell accumulation, and survival of grafted hPSC-derived DA neurons.[30] A study of transplanting hiPSC-derived MSCs into the thyroid cartilage also showed no significant difference in engraftment of hiPSC-cartilage tissues between X-SCID and nude rats although these results were not obtained from a single study.[31,32] In our results, hiPSC-AE showed a non-significant trend ~~trend toward higher engraftment efficiency~~ in X-SCID rats, and hiPSC-derived mesenchymal cells showed higher engraftment efficiency in X-SCID rats, showing statistical significance. These results suggest that immunosuppression of recipient rats affects the engraftment efficiency in hiPSC-AE and hiPSC-

derived mesenchymal cells. Epithelial cells are subjected to stimuli such as airflow in respiration after transplantation, their engraftment efficiency was low and varied widely, and no statistically significant difference was obtained in this study. In the future, a significant difference may be confirmed by increasing the number of experiments. However, as mesenchymal cells in the mesenchymal tissue free from ambient stimuli show higher engraftment potency, they may have shown statistically significant differences. In the present study, mesenchymal cells are non-objective cells of differentiation from hiPSCs and transplantation; however, the results of this study are important to the transplantation of hiPSC-derived mesenchymal cells for the establishment of trachea-humanized rats in the future.

The immunosuppression of the two strains of recipient rats was also investigated. T cells are considered nearly non-existent in both nude and X-SCID rats, as expected, and the number of pan T-cell marker CD3-positive cells that accumulated in the graft area showed no difference in both strains. CD45, known as a leukocyte common antigen, is expressed in most nucleated cells with hematopoietic origin, and MHC class II molecules are expressed on macrophages, dendritic cells, activated T cells, and B cells. The abundance of CD45-positive and MHC class II-positive cells accumulating in the graft area was significantly lower in X-SCID rats, which lack T, B, and NK cells. These results suggest the possibility that the engraftment efficiency of hiPSC-derived cells may have been increased using X-SCID rats with extremely suppressed immune responses. In a study in which the same AE cells were transplanted into the middle ear, engraftment on the luminal surface failed in nude rats, whereas it succeeded in X-SCID rats.[33] Since brain and cartilage have immune privilege,[34,35] the engraftment efficiency in hiPSC-derived cell transplantation into these tissues was not different[30–32]; however, the airway epithelium may show differences in immunosuppression and consequently in engraftment efficiency.

The engraftment efficiency did not increase as expected in this study. This may suggest that other factors should be considered in addition to the strain of the recipient animals. A possible factor is the use of collagen vitrigel membrane[36] as a scaffold. In a previous study and the present study, we used commercially available bovine collagen vitrigel membranes for the preparation of cell sheets.[8] At this time, we also used porcine atelocollagen vitrigel membranes with low antigenicity and compared the

engraftment efficiency in hiPSC-AE transplantation in nude rats (Fig. S1); however, no differences were observed. The median percentages of the porcine atelocollagen vitrigel membrane group and the bovine collagen vitrigel membrane group were 2.16% (0.09%–10.16%) and 1.78% (0.21%–5.32%) (porcine atelocollagen vitrigel membrane, n = 5; bovine collagen vitrigel membrane, n = 5), respectively. Various other factors such as the treatment with growth factors and small molecules for the promotion of engraftment or differentiation stage of the transplanted cells are also conceivable. For clinical studies, to avoid the immune response by the depletion of antigen expression in transplanted cells, HLA depletion has been considered.[37,38] Therefore, genome-edited hiPSCs lacking proteins involving immune response to xenotransplantation may be useful, as reported in xenotransplantation using non-human primates and pigs.[39] Furthermore, our previous study indicated that transplanted hiPSC-AE formed a polarized thicker epithelia with an AcTub-positive cilia-like structure in the apical surface at 1 week after transplantation, without significant differences in the proportion of surviving cells in the epithelia of the transplanted site at 1 and 2 weeks (Okuyama et al., 2019); thus, we defined our experimental period as 2 weeks. However, to observe surviving cells and immune cell responses, long-term evaluation should also be conducted in future research.

In conclusion, to establish a trachea-humanized rat model by improving engraftment efficiency, we compared the engraftment efficiency and immune response in nude and X-SCID rats transplanted with hiPSC-AE into tracheae. The engraftment efficiency of epithelial cells tended to be high in X-SCID rats, although no statistical difference was found, whereas the engraftment efficiency of mesenchymal cells was higher than that in X-SCID rats. Furthermore, the number of immune cells accumulated in the grafted area showed that pan T-cell marker CD3-positive cells did not differ between the two strains; however, the abundance of CD45-positive and MHC class II-positive cells significantly decreased in X-SCID rats. These results indicate that X-SCID rats are more useful for the transplantation of hiPSC-AE into tracheae to generate trachea-humanized rat models.

Acknowledgments

The electron microscopy study was supported by the Division of Electron Microscopic Study,

Center for Anatomical Studies, Graduate School of Medicine, Kyoto University.

Author contributions

Y. Kishimoto, H. Ohnishi, and K. Omori designed the study. Y. Hayashi and H. Ohnishi prepared hiPSC-derived AEs and graft. Y. Hayashi, H. Okuyama and M. Kitano performed the transplantation. Y. Hayashi, H. Ohnishi, M. Kitano, M. Yoshimatsu, F. Kuwata, T. Tada, and K. Mizuno performed the histological and data analyses. T. Takezawa prepared culture inserts with atelocollagen vitrigel membrane. Y. Hayashi, H. Ohnishi, and Y. Kishimoto wrote the main manuscript and create the figures and table. All authors approved the final manuscript.

Conflict of interest

The authors declare no competing interests.

Funding statement

This work was supported by the Japan Society for the Promotion of Science (JSPS) KAKENHI (22K09666) and alumni otolaryngology fund from the Department of Otolaryngology–Head and Neck Surgery, Graduate School of Medicine, Kyoto University.

References

1. Takahashi K, Tanabe K, Ohnuki M, et al. Induction of pluripotent stem cells from adult human fibroblasts by defined factors. *Cell*. Nov 2007;131(5):861-72. doi:10.1016/j.cell.2007.11.019
2. Mandai M, Kurimoto Y, Takahashi M. Autologous Induced Stem-Cell-Derived Retinal Cells for Macular Degeneration. *N Engl J Med*. Aug 24 2017;377(8):792-793. doi:10.1056/NEJMc1706274
3. Takahashi J. iPS cell-based therapy for Parkinson's disease: A Kyoto trial. *Regen Ther*. Mar 2020;13:18-22. doi:10.1016/j.reth.2020.06.002
4. Sugimoto N, Kanda J, Nakamura S, et al. iPLAT1: the first-in-human clinical trial of iPSC-derived platelets as a phase 1 autologous transfusion study. *Blood*. Dec 01 2022;140(22):2398-2402. doi:10.1182/blood.2022017296

5. Miyagawa S, Kainuma S, Kawamura T, et al. Case report: Transplantation of human induced pluripotent stem cell-derived cardiomyocyte patches for ischemic cardiomyopathy. *Front Cardiovasc Med*. 2022;9:950829. doi:10.3389/fcvm.2022.950829

6. Yu F, Liu F, Liang X, et al. iPSC-Derived Airway Epithelial Cells: Progress, Promise, and Challenges. *Stem Cells*. Jan 30 2023;41(1):1-10. doi:10.1093/stmcls/sxac074

7. Konishi S, Gotoh S, Tateishi K, et al. Directed Induction of Functional Multi-ciliated Cells in Proximal Airway Epithelial Spheroids from Human Pluripotent Stem Cells. *Stem Cell Reports*. Jan 2016;6(1):18-25. doi:10.1016/j.stemcr.2015.11.010

8. Okuyama H, Ohnishi H, Nakamura R, et al. Transplantation of multiciliated airway cells derived from human iPS cells using an artificial tracheal patch into rat trachea. *Journal of Tissue Engineering and Regenerative Medicine*. Jun 2019;13(6):1019-1030. doi:10.1002/term.2849

9. Festing MF, May D, Connors TA, Lovell D, Sparrow S. An athymic nude mutation in the rat. *Nature*. Jul 27 1978;274(5669):365-6. doi:10.1038/274365a0

10. Miyasaka Y, Wang J, Hattori K, et al. A high-quality severe combined immunodeficiency (SCID) rat bioresource. *PLoS One*. 2022;17(8):e0272950. doi:10.1371/journal.pone.0272950

11. Leonard WJ, Noguchi M, Russell SM, McBride OW. The molecular basis of X-linked severe combined immunodeficiency: the role of the interleukin-2 receptor gamma chain as a common gamma chain, gamma c. *Immunol Rev*. Apr 1994;138:61-86. doi:10.1111/j.1600-065x.1994.tb00847.x

12. Nakagawa M, Koyanagi M, Tanabe K, et al. Generation of induced pluripotent stem cells without Myc from mouse and human fibroblasts. *Nat Biotechnol*. Jan 2008;26(1):101-6. doi:10.1038/nbt1374

13. Gotoh S, Ito I, Nagasaki T, et al. Generation of alveolar epithelial spheroids via isolated progenitor cells from human pluripotent stem cells. *Stem Cell Reports*. Sep 2014;3(3):394-403. doi:10.1016/j.stemcr.2014.07.005

14. Lu T, Yang B, Wang R, Qin C. Xenotransplantation: Current Status in Preclinical Research. *Front Immunol*. 2019;10:3060. doi:10.3389/fimmu.2019.03060

15. Puga Yung G, Schneider MK, Seebach JD. Immune responses to alpha1,3 galactosyltransferase knockout pigs. *Curr Opin Organ Transplant*. Apr 2009;14(2):154-60. doi:10.1097/MOT.0b013e328329250d

16. Sommaggio R, Bello-Gil D, Pérez-Cruz M, Brokaw JL, Máñez R, Costa C. Genetic engineering strategies to prevent the effects of antibody and complement on xenogeneic chondrocytes. *Eur Cell Mater*. Nov 18 2015;30:258-70. doi:10.22203/ecm.v030a18

17. Ding JW, Zhou T, Ma L, et al. Expression of complement regulatory proteins in accommodated xenografts induced by anti-alpha-Gal IgG1 in a rat-to-mouse model. *Am J Transplant*. Jan 2008;8(1):32-40. doi:10.1111/j.1600-6143.2007.02016.x

18. Maeda A, Kogata S, Toyama C, et al. The Innate Cellular Immune Response in Xenotransplantation. *Front Immunol*. 2022;13:858604. doi:10.3389/fimmu.2022.858604

19. Yang X, Zhou J, He J, et al. An Immune System-Modified Rat Model for Human Stem Cell Transplantation Research. *Stem Cell Reports*. Aug 14 2018;11(2):514-521. doi:10.1016/j.stemcr.2018.06.004

20. Miyakawa Y, Ohnishi Y, Tomisawa M, et al. Establishment of a new model of human multiple myeloma using NOD/SCID/gammac(null) (NOG) mice. *Biochem Biophys Res Commun*. Jan 09 2004;313(2):258-62. doi:10.1016/j.bbrc.2003.11.120

21. Kenney LL, Shultz LD, Greiner DL, Brehm MA. Humanized Mouse Models for Transplant Immunology. *Am J Transplant*. Feb 2016;16(2):389-97. doi:10.1111/ajt.13520

22. Mashimo T, Takizawa A, Kobayashi J, et al. Generation and characterization of severe combined immunodeficiency rats. *Cell Rep*. Sep 27 2012;2(3):685-94. doi:10.1016/j.celrep.2012.08.009

23. Mashimo T, Takizawa A, Voigt B, et al. Generation of knockout rats with X-linked severe combined immunodeficiency (X-SCID) using zinc-finger nucleases. *PLoS One*. Jan 25 2010;5(1):e8870. doi:10.1371/journal.pone.0008870

24. Hashikawa Y, Hayashi R, Tajima M, et al. Generation of knockout rabbits with X-linked severe combined immunodeficiency (X-SCID) using CRISPR/Cas9. *Sci Rep*. Jun 19 2020;10(1):9957. doi:10.1038/s41598-020-66780-6

25. Suzuki S, Iwamoto M, Saito Y, et al. Il2rg gene-targeted severe combined immunodeficiency pigs. *Cell Stem Cell*. Jun 14 2012;10(6):753-758. doi:10.1016/j.stem.2012.04.021

26. Sato K, Oiwa R, Kumita W, et al. Generation of a Nonhuman Primate Model of Severe Combined Immunodeficiency Using Highly Efficient Genome Editing. *Cell Stem Cell*. Jul 07 2016;19(1):127-38. doi:10.1016/j.stem.2016.06.003

27. Segre JA, Nemhauser JL, Taylor BA, Nadeau JH, Lander ES. Positional cloning of the nude locus: genetic, physical, and transcription maps of the region and mutations in the mouse and rat. *Genomics*. Aug 10 1995;28(3):549-59. doi:10.1006/geno.1995.1187

28. Vos JG, Kreeftenberg JG, Kruijt BC, Kruizinga W, Steerenberg P. The athymic nude rat. II. Immunological characteristics. *Clin Immunol Immunopathol*. Feb 1980;15(2):229-37. doi:10.1016/0090-1229(80)90033-1

29. Leonard WJ. Cytokines and immunodeficiency diseases. *Nat Rev Immunol*. Dec 2001;1(3):200-8. doi:10.1038/35105066

30. Samata B, Kikuchi T, Miyawaki Y, et al. X-linked severe combined immunodeficiency (X-SCID) rats for xeno-transplantation and behavioral evaluation. *J Neurosci Methods*. Mar 30 2015;243:68-77. doi:10.1016/j.jneumeth.2015.01.027

31. Yoshimatsu M, Ohnishi H, Zhao C, et al. In vivo regeneration of rat laryngeal cartilage with mesenchymal stem cells derived from human induced pluripotent stem cells via neural crest cells. *Stem Cell Res*. Apr 2021;52:102233. doi:10.1016/j.scr.2021.102233

32. Mizuno K, Ohnishi H, Yoshimatsu M, et al. Laryngeal Cartilage Regeneration of Nude Rats by Transplantation of Mesenchymal Stem Cells Derived from Human-Induced Pluripotent Stem Cells. *Cell Transplant*. 2023;32:9636897231178460. doi:10.1177/09636897231178460

33. Tada T, Ohnishi H, Yamamoto N, et al. Transplantation of a human induced pluripotent stem cell-derived airway epithelial cell sheet into the middle ear of rats. *Regen Ther*. Mar 2022;19:77-87. doi:10.1016/j.reth.2022.01.001

34. Revell CM, Athanasiou KA. Success rates and immunologic responses of autogenic, allogenic, and xenogenic treatments to repair articular cartilage defects. *Tissue Eng Part B Rev*. Mar 2009;15(1):1-15. doi:10.1089/ten.teb.2008.0189

35. Mapunda JA, Tibar H, Regragui W, Engelhardt B. How Does the Immune System Enter the Brain? *Front Immunol*. 2022;13:805657. doi:10.3389/fimmu.2022.805657

36. Takezawa T, Ozaki K, Nitani A, Takabayashi C, Shimo-Oka T. Collagen vitrigel: a novel scaffold that can facilitate a three-dimensional culture for reconstructing organoids. *Cell Transplant*. 2004;13(4):463-73. doi:10.3727/000000004783983882

37. Koga K, Wang B, Kaneko S. Current status and future perspectives of HLA-edited induced pluripotent stem cells. *Inflamm Regen*. 2020;40:23. doi:10.1186/s41232-020-00132-9

38. Otsuka R, Wada H, Murata T, Seino KI. Immune reaction and regulation in transplantation based on pluripotent stem cell technology. *Inflamm Regen*. 2020;40:12. doi:10.1186/s41232-020-00125-8

39. Platt JL, Cascalho M, Piedrahita JA. Xenotransplantation: Progress Along Paths Uncertain from Models to Application. *ILAR J*. Dec 31 2018;59(3):286-308. doi:10.1093/ilar/ily015

40. Aoki S, Sakata Y, Shimoda R, et al. High-density collagen patch prevents stricture after endoscopic circumferential submucosal dissection of the esophagus: a porcine model. *Gastrointest Endosc*. May 2017;85(5):1076-1085. doi:10.1016/j.gie.2016.10.012

41. Aoki S, Takezawa T, Ikeda S, et al. A new cell-free bandage-type artificial skin for cutaneous wounds. *Wound Repair Regen*. 2015;23(6):819-29. doi:10.1111/wrr.12321

Figure legends

Fig. 1. Preparation of graft. (A) Immunofluorescent staining of apical surfaces of induced cells on day 56. The expressions of E-cadherin (green) and AcTub (red) were observed. Scale bar = 50 µm. (B, C) Immunofluorescent staining of a vertical section of an induced cell sheet on day 56. KRT5 (B) and MUC5AC (C) expression were observed. Scale bars = 50 µm. (D) A vertical section of induced cells observed by transmission electron microscopy on day 56. The inset shows the "9 + 2" structure in cilia-like protrusions, which is the specific structure of motile cilia. Scale bar = 10 µm. ~~Cilia-like protrusions on the apical surface of induced cells were observed by scanning electron microscopy on day 56. Scale bar = 30 µm.~~ (~~C~~E) Cilia-like protrusions on the apical surface of induced cells were observed by scanning electron microscopy on day 56. Scale bar = 30 µm. ~~A vertical section of induced cells observed by transmission electron microscopy on day 56. The inset shows the "9 + 2" structure in cilia-like protrusions, which is the specific structure of motile cilia. Scale bar = 10 µm.~~ (~~D~~F) An artificial trachea used as a scaffold. Stumps of polypropylene mesh are found between the collagen sponge. Scale bar = 300 µm. AcTub, acetylated α-tubulin; KRT5, cytokeratin5; MUC5AC, Mucin5AC ~~(MUC5AC)~~; DAPI, 4',6 - diamidino-2-phenylindole.

Fig. 2. Transplantation of an artificial trachea covered with an hiPSC-AE sheet. (A) Schema of the experimental design. (B) Axial section of a nude rat trachea including the transplanted area. The proportion of hiPSC-derived epithelia in the total epithelia at the transplanted area was calculated from two epithelial areas with a width of 350 µm at the center and one side of the tracheal defect area (two yellow squares). The proportion of hiPSC-derived mesenchymal cell was calculated from the HNA-positive area and grafted area (area surrounded by a yellow dotted line). hiPSC-AE, human iPSC-derived airway epithelia; HNA, human nuclear antigen; DAPI, 4′,6-diamidino-2-phenylindole.

Fig. 3. Survived cells in the tracheal epithelia. (A) Immunofluorescent staining images of the transplanted area including the surviving transplanted cells in a nude rat (a–c) and X-SCID rat (d–f). Some hiPSC-derived HNA-positive cells (b, e) were positive for the ciliated cell marker AcTub (c, f).

Phalloidin shows the outline of the cells in tracheae, and DAPI was used as a counterstain. Scale bar = 100 μm. Yellow arrowheads show the hiPSC-derived ciliated cells. (B) Comparison of the proportion of the HNA-positive epithelia in the total epithelia in nude and X-SCID ($p = 0.347$, Mann–Whitney U test) rats (nude rats, $n = 5$; X-SCID rats, $n = 5$). DAPI, 4′,6-diamidino-2-phenylindole; hiPSC-AE, human iPSC-derived airway epithelia; HNA, human nuclear antigen; X-SCID, X-linked severe combined immunodeficiency.

Fig. 4. Survived cells in the mesenchymal tissues in tracheae. (A) Shema of the area used for the calculation of the proportion of HNA-positive cells in the grafted area. (B) Immunofluorescent staining images of the transplanted area including the surviving transplanted cells in a nude rat (a–c) and X-SCID rat (d–f). In the grafts, hiPSC-derived HNA-positive areas (a, d) are observed. Phalloidin shows the outline of the cells in tracheae (b, e). Merged images. (c, f) Scale bar = 500 μm. (C) Comparison of the proportion of HNA-positive areas in grafts in nude and X-SCID ($p = 0.021$, Mann–Whitney U test) rats (nude rats, $n = 8$; X-SCID rats, $n = 8$). DAPI, 4′,6-diamidino-2-phenylindole; HNA, human nuclear antigen; X-SCID, X-linked severe combined immunodeficiency.

Fig. 5. Immune response in the transplantation site. (A) Representative images of the three types of immune cells in wild-type, nude, and X-SCID rats. Scale bar = 20 μm. (B) Comparison of the numbers of the three types of immune cells in grafts in nude and X-SCID rats (CD3, CD45, and MHC class II, $p = 0.674$, 0.005, and 0.009, Mann–Whitney U test) (nude rats, $n = 8$; X-SCID rats, $n = 8$). WT, wild-type rats; nude, nude rats; X-SCID, X-linked severe combined immunodeficiency rats.

Table 1. Antibodies used in this study

Antibody	Manufacturer (Catalog No.)	dilution
Anti Acetylated Tubulin antibody	Sigma (A-10042)	1:1000
Anti-E-cadherin antibody	TAKARA (ECCD2)	1:2000
Anti Keratin 5 antibody	BioLegend, 905501	1:1000
Anti MUC5AC antibody	Bioss Antibodies Inc., bs-7166R	1:1000
Anti-human nuclei antigen antibody	Millipore (MAB1281)	1:1000
Anti-CD3 antibody	Abcam (ab5690)	1:1000
Anti-CD45 antibody	BD biosciences (550566)	1:1000
Anti-MHC class II antibody	Abcam (ab23990)	1:200

Figure.1

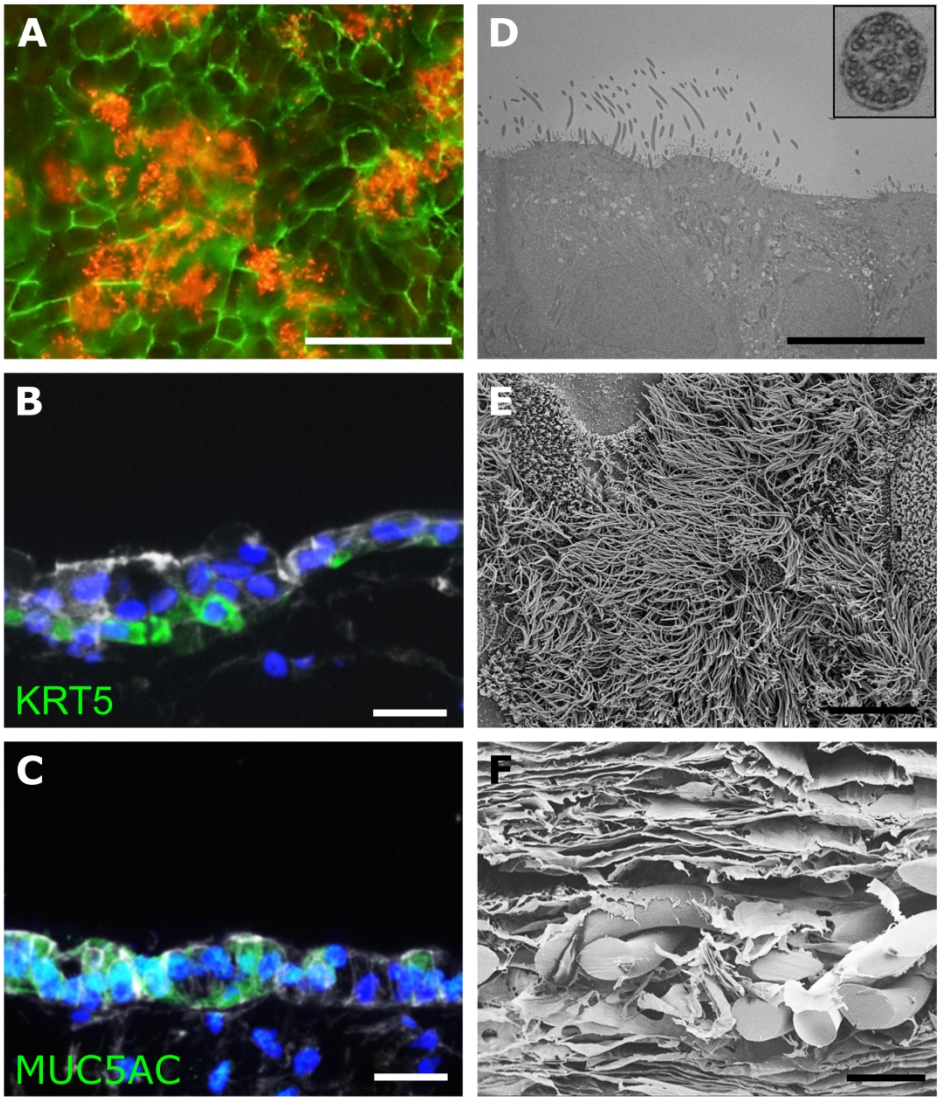

Preparation of graft. (A) Immunofluorescent staining of apical surfaces of induced cells on day 56. The expressions of E-cadherin (green) and AcTub (red) were observed. Scale bar = 50 μm. (B, C) Immunofluorescent staining of a vertical section of an induced cell sheet on day 56. KRT5 (B) and MUC5AC (C) expression were observed. Scale bars = 50 μm. (D) A vertical section of induced cells observed by transmission electron microscopy on day 56. The inset shows the "9 + 2" structure in cilia-like protrusions, which is the specific structure of motile cilia. Scale bar = 10 μm. (E) Cilia-like protrusions on the apical surface of induced cells were observed by scanning electron microscopy on day 56. Scale bar = 30 μm. (F) An artificial trachea used as a scaffold. Stumps of polypropylene mesh are found between the collagen sponge. Scale bar = 300 μm. AcTub, acetylated α-tubulin; KRT5, cytokeratin5; MUC5AC, Mucin5AC; DAPI, 4',6 - diamidino-2-phenylindole.

532x662mm (118 x 118 DPI)

Figure.2

A

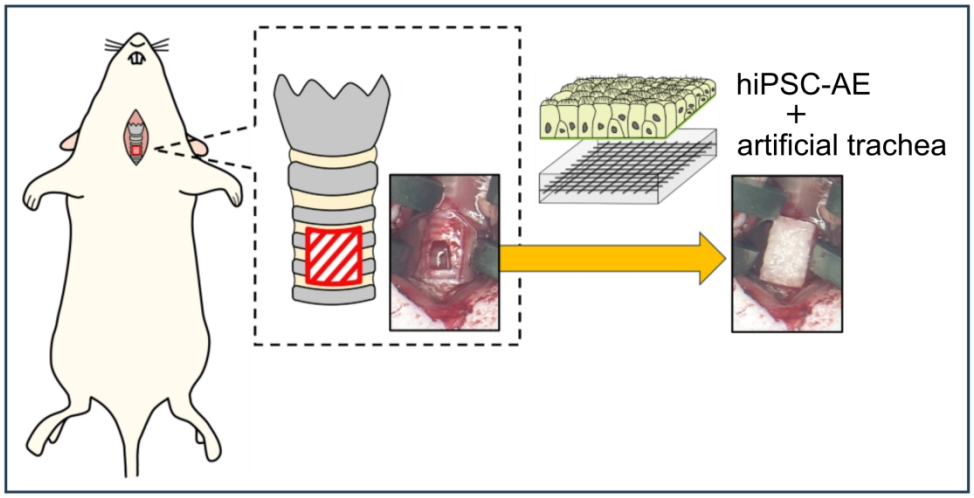

B

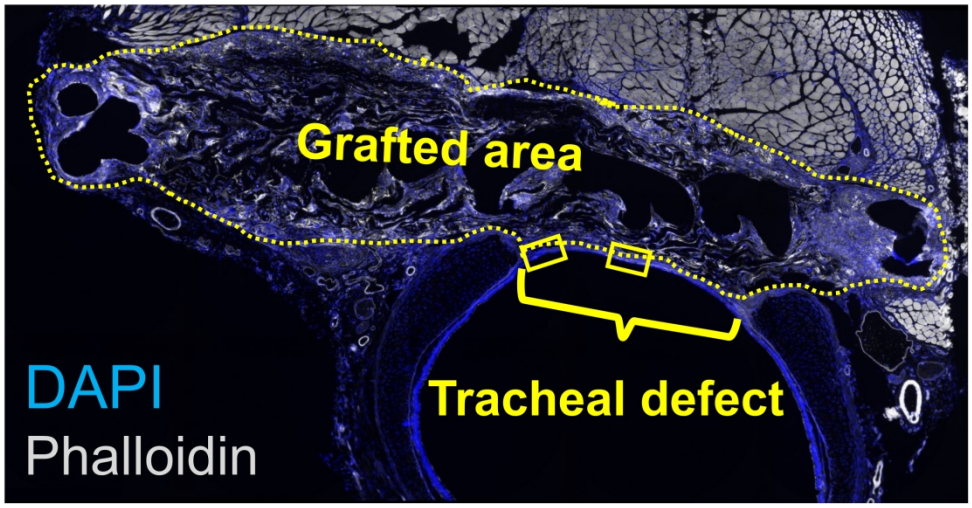

Transplantation of an artificial trachea covered with an hiPSC-AE sheet. (A) Schema of the experimental design. (B) Axial section of a nude rat trachea including the transplanted area. hiPSC-AE, human iPSC-derived airway epithelia. The proportion of hiPSC-derived epithelia in the total epithelia at the transplanted area was calculated from two epithelial areas with a width of 350 μm at the center and one side of the tracheal defect area (two yellow squares). The proportion of hiPSC-derived mesenchymal cell was calculated from the HNA-positive area and grafted area (area surrounded by a yellow dotted line). DAPI, 4′,6-diamidino-2-phenylindole.

527x645mm (118 x 118 DPI)

Figure.3

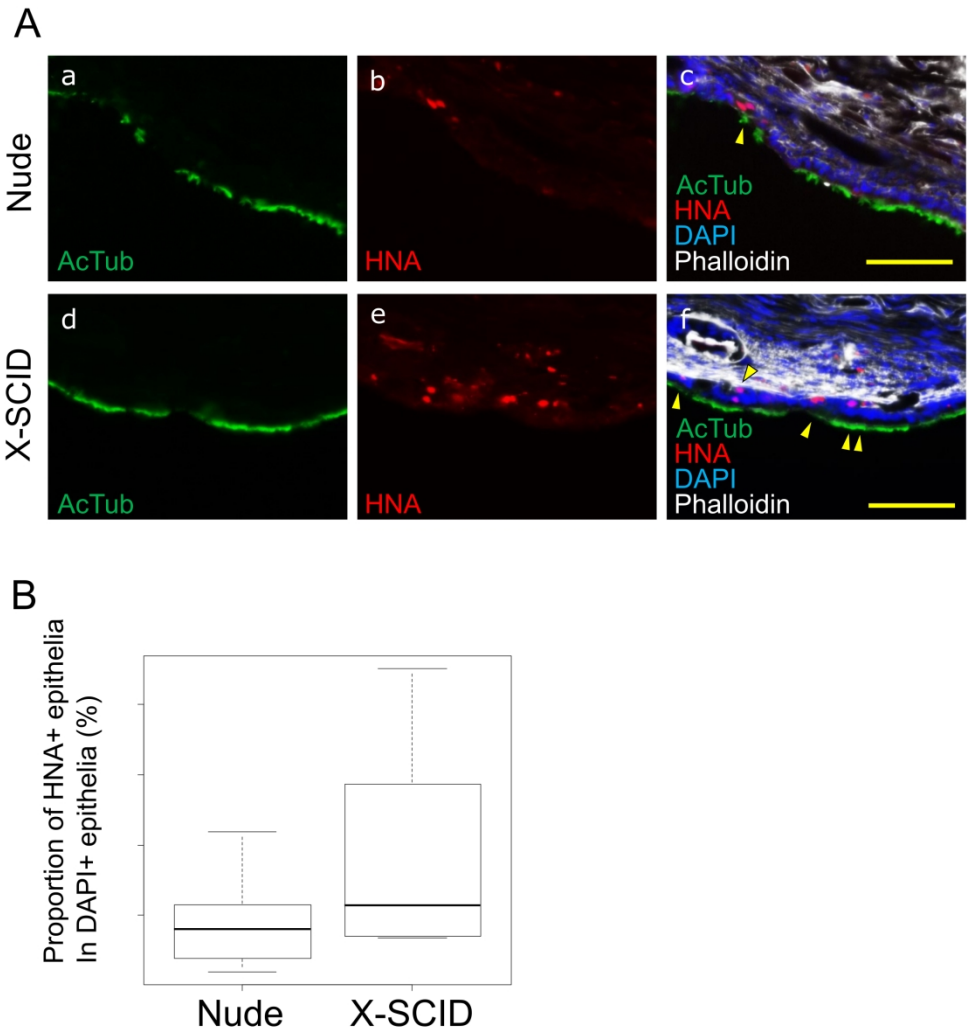

Survived cells in the tracheal epithelia. (A) Immunofluorescent staining images of the transplanted area including the surviving transplanted cells in a nude rat (a–c) and X-SCID rat (d–f). Some hiPSC-derived HNA-positive cells (b, e) were positive for the ciliated cell marker AcTub (c, f). Phalloidin shows the outline of the cells in tracheae, and DAPI was used as a counterstain. Scale bar = 100 μm. Yellow arrowheads show the hiPSC-derived ciliated cells. (B) Comparison of the proportion of the HNA-positive epithelia in the total epithelia in nude and X-SCID (p = 0.347, Mann–Whitney U test) rats (nude rats, n = 5; X-SCID rats, n = 5). DAPI, 4′,6-diamidino-2-phenylindole; hiPSC-AE, human iPSC-derived airway epithelia; HNA, human nuclear antigen; X-SCID, X-linked severe combined immunodeficiency.

534x611mm (116 x 116 DPI)

Figure.4

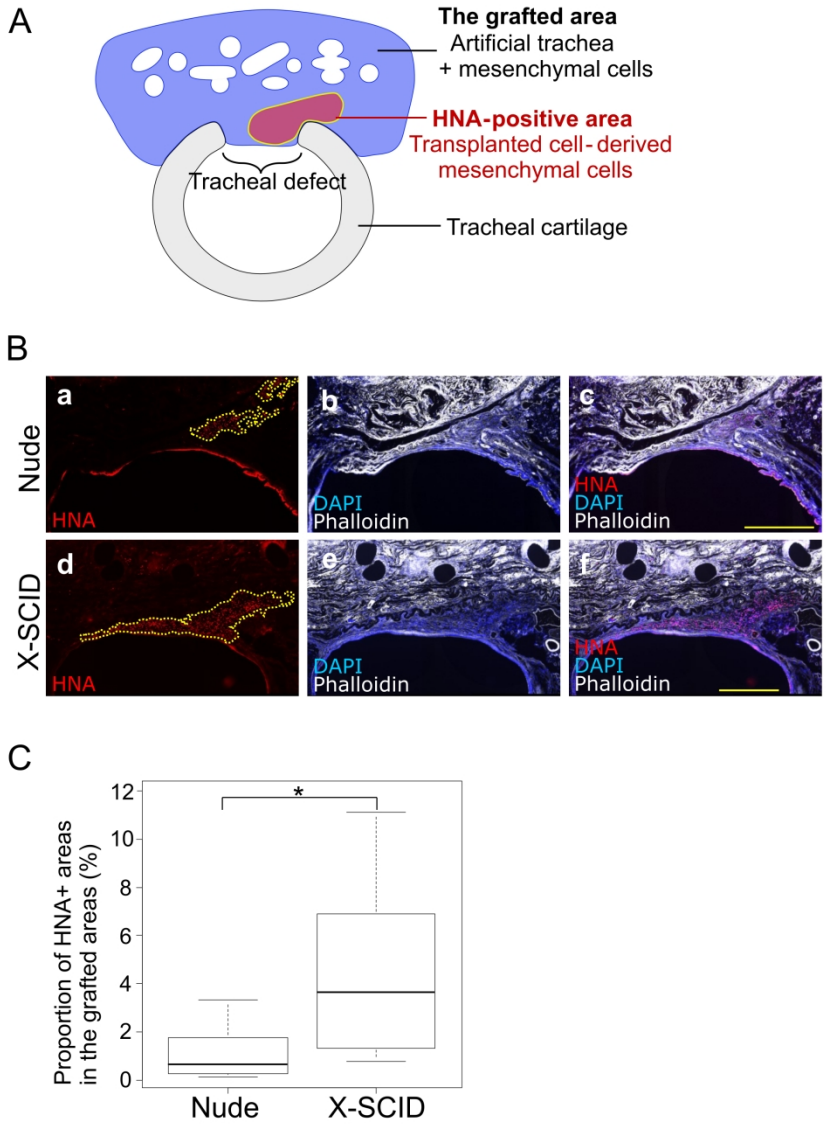

Survived cells in the mesenchymal tissues in tracheae. (A) Shema of the area used for the calculation of the proportion of HNA-positive cells in the grafted area. (B) Immunofluorescent staining images of the transplanted area including the surviving transplanted cells in a nude rat (a–c) and X-SCID rat (d–f). In the grafts, hiPSC-derived HNA-positive areas (a, d) are observed. Phalloidin shows the outline of the cells in tracheae (b, e). Merged images. (c, f) Scale bar = 500 μm. (C) Comparison of the proportion of HNA-positive areas in grafts in nude and X-SCID ($p = 0.021$, Mann–Whitney U test) rats (nude rats, $n = 8$; X-SCID rats, $n = 8$). DAPI, 4′,6-diamidino-2-phenylindole; HNA, human nuclear antigen; X-SCID, X-linked severe combined immunodeficiency.

532x746mm (118 x 118 DPI)

Figure.5

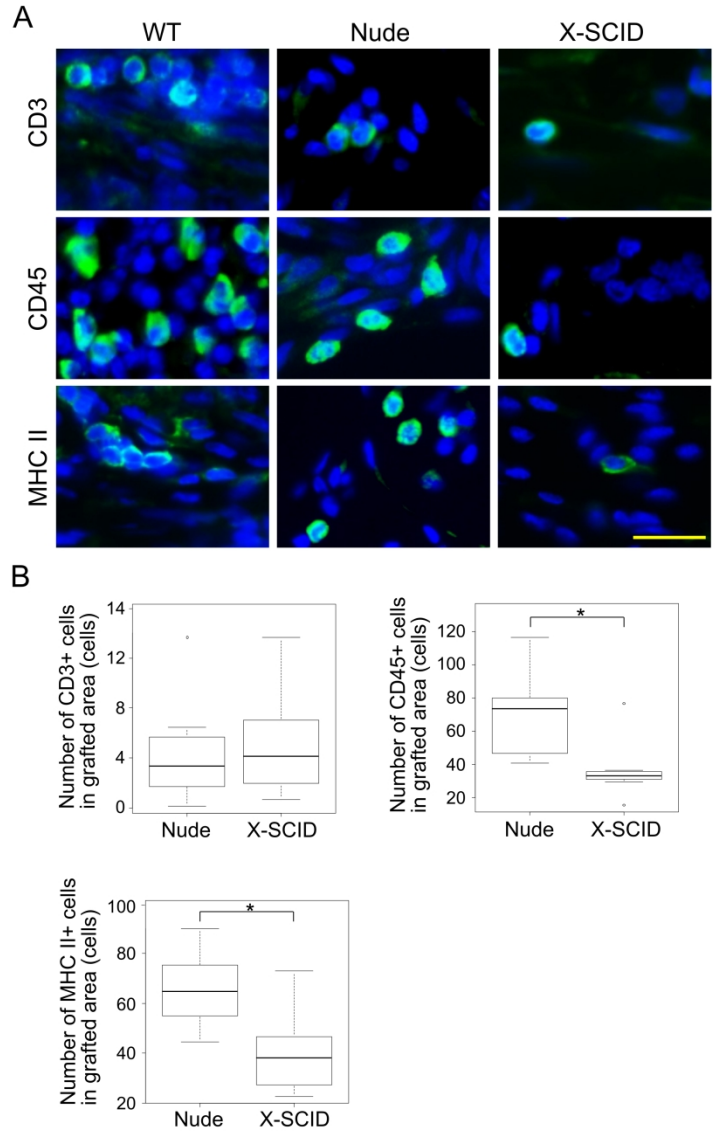

Immune response in the transplantation site. (A) Representative images of the three types of immune cells in wild-type, nude, and X-SCID rats. Scale bar = 20 μm. (B) Comparison of the numbers of the three types of immune cells in grafts in nude and X-SCID rats (CD3, CD45, and MHC class II, p = 0.674, 0.005, and 0.009, Mann–Whitney U test) (nude rats, n = 8; X-SCID rats, n = 8). WT, wild-type rats; nude, nude rats; X-SCID, X-linked severe combined immunodeficiency rats.

531x855mm (118 x 118 DPI)

Supplemental material

Supplementary materials and methods

The 0.5% atelocollagen solution was prepared by uniformly mixing equal volumes of 1.0% acidic solution of porcine-derived collagen formulated for regenerative medicine (Kanto Chemical) and serum-free DMEM containing 20 mM N-2-hydroxyethylpiperazine-N'-2-ethanesulfonic acid, 100 U/mL penicillin, and 100 μg/mL streptomycin (Thermo Fisher Scientific). A collagen vitrigel membrane containing 2.2-mg collagen/cm^2 unit area was fabricated by gelation, vitrification, and rehydration with PBS, as previously described.[40,41] Then, the membrane was converted into an atelocollagen xerogel membrane by revitrification on a separable sheet. The xerogel membrane was pasted onto the bottom-side edge of a plastic cylinder (inner–outer diameter of 11–15 mm) and a length of 15 mm, and a couple of hangers were connected to its top edge of the cylinder. These cell culture inserts with a porcine atelocollagen xerogel membrane, which could be easily converted into an atelocollagen vitrigel membrane by rehydration, were used to prepare hiPSC-AE sheets.

Supplementary figure legend

Supplementary Fig. S1. Comparison of the proportion of HNA-positive epithelia in the total epithelia in the grafted area in the porcine atelocollagen vitrigel membrane group and the bovine collagen vitrigel membrane group (p = 1, Mann–Whitney U test). The median percentages of the porcine atelocollagen vitrigel membrane group and the bovine collagen vitrigel membrane group were 2.16% (0.09%–10.16%) and 1.78% (0.21%–5.32%) (porcine atelocollagen vitrigel membrane, n = 5; bovine collagen vitrigel membrane, n = 5), respectively. DAPI, 4′,6-diamidino-2-phenylindole; HNA, human nuclear antigen.

Figure.S1

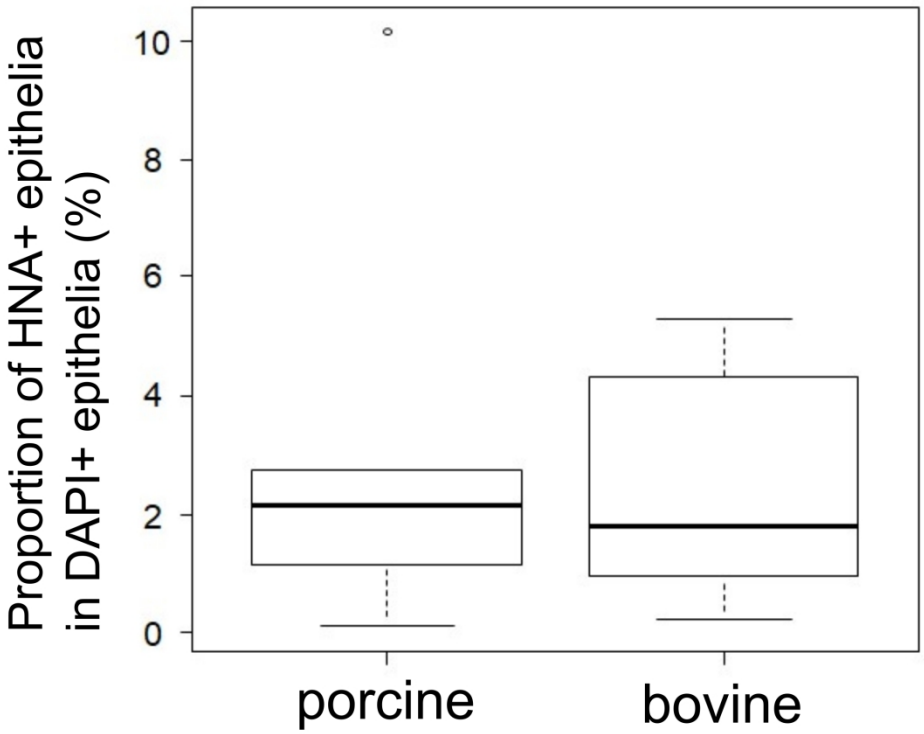

Comparison of the proportion of HNA-positive epithelia in the total epithelia in the grafted area in the porcine atelocollagen vitrigel membrane group and the bovine collagen vitrigel membrane group (p = 1, Mann–Whitney U test). The median percentages of the porcine atelocollagen vitrigel membrane group and the bovine collagen vitrigel membrane group were 2.16% (0.09%–10.16%) and 1.78% (0.21%–5.32%) (porcine atelocollagen vitrigel membrane, n = 5; bovine collagen vitrigel membrane, n = 5), respectively. DAPI, 4′,6-diamidino-2-phenylindole; HNA, human nuclear antigen.

529x504mm (118 x 118 DPI)